ELSEVIER

MCN Molecular and Cellular Neuroscience

www.elsevier.com/locate/ymcne
Mol. Cell. Neurosci. 25 (2004) 383–393

Regulation of caspase activation in axotomized retinal ganglion cells

Zelda H. Cheung,[a] Yuen-Man Chan,[a,b] Flora K.W. Siu,[c] Henry K. Yip,[a,b] Wutian Wu,[a,b] Mason C.P. Leung,[c] and Kwok-Fai So[a,b,*]

[a] *Department of Anatomy, Faculty of Medicine, The University of Hong Kong, Hong Kong, China*
[b] *Central Lab of the Institute of Molecular Technology for Drug Discovery and Synthesis, The University of Hong Kong, China*
[c] *Department of Rehabilitation Sciences, The Hong Kong Polytechnic University, Hong Kong, China*

Received 21 November 2002; revised 22 October 2003; accepted 5 November 2003

Transection of the optic nerve initiates massive death of retinal ganglion cells (RGCs). Interestingly, despite the severity of the injury, RGC loss was not observed until several days after axotomy. The mechanisms responsible for this initial lack of RGC death remained unknown. In the current study, immunohistochemical analysis revealed that caspases-3 and -9 activation in the RGCs were not detected until day 3 post-axotomy, coinciding with the onset of axotomy-induced RGC loss. Interestingly, elevated Akt phosphorylation was observed in axotomized retinas during the absence of caspase activation. Inhibiting the increase in Akt phosphorylation by intravitreal injection of wortmannin and LY294002, inhibitors of PI3K, resulted in premature nuclear fragmentation, caspases-3 and -9 activation in the ganglion cell layer. Our findings thus indicate that the PI3K/Akt pathway may serve as an endogenous regulator of caspase activation in axotomized RGCs, thereby, contributing to the late onset of RGC death following axotomy.

Introduction

Transection of the optic nerve results in the death of retinal ganglion cells (RGCs) (Berkelaar et al., 1994; Peinado-Ramon et al., 1996). Axotomy-induced RGC death is only noticeable at 4 days post-axotomy (dpa) in adult rats (Berkelaar et al., 1994; Koeberle and Ball, 1998). Rapid RGC death then continues until 7 dpa, when axotomized RGC death enters a slower elimination phase (Koeberle and Ball, 1998; Takano and Horie, 1994; Villegas-Perez et al., 1993). By 14 dpa, not more than 10–20% of the axotomized RGCs remains (Berkelaar et al., 1994). While the temporal profile of axotomized RGC death has been rather well characterized, the molecular mechanisms controlling the kinetics of axotomized RGC death remain elusive. In particular, little is known concerning the mechanisms underlying the observed delay between axonal injury and the death of axotomized RGCs. Recently, morphological and biochemical analyses suggest that axotomized RGCs die via an apoptotic pathway. Western blot analyses demonstrated that caspase-3 and -9 are activated in axotomized rat retina (Kermer et al., 1999, 2000a). In addition, intravitreal injections of caspase-3- and -9-specific inhibitors significantly enhances RGC survival at 14 dpa (Chaudhary et al., 1999; Kermer et al., 1998, 2000a), indicating that the activation of these two caspases is involved in the demise of the damaged neurons. This suggests that the kinetics of caspase activation, and pathways participating in the regulation of caspase activation, may affect the rate of axotomized RGC death. Therefore, the aim of the current study is to elucidate the molecular events contributing to the late onset of detectable axotomized RGC death by examining the kinetics of caspase activation, and the mechanisms implicated in the regulation of caspase activation.

In this study, we found that axotomized RGC death commenced at 3 dpa in adult hamsters. Interestingly, activation of caspase-3 and -9 in axotomized RGCs coincided with the late detection of axotomized RGC death and was similarly not observed until 3 dpa. The concomitant onset of caspase activation and RGC death indicates that the late activation of caspases may contribute the initial lack of RGC death following axotomy. We thus went on to examine the mechanisms of this delayed activation of caspases, and if the delayed caspases activation contributed to the late detection of axotomized RGC death. Recent reports indicate that activation of the PI3K/Akt pathway serves as important survival signals (Barber et al., 2001; Dudek et al., 1997; Nunez and del Peso, 1998; Politi et al., 2001). Akt is activated following phosphorylation at Serine 473 and Threonine 308 after PI3K activation (O'Gorman and Cotter, 2001). Activated Akt then exerts its anti-apoptotic effect by phosphorylating multiple targets downstream. Akt has been demonstrated to inhibit Bad to limit cytochrome *c* release (Datta et al., 1997), in addition to displaying inhibitory effect on activated caspase-9 (Cardone et al., 1998; Zhou et al., 2000). The PI3K/Akt pathway therefore presents a potential candidate for regulating caspase activation in axotomized RGCs. In the current study, we examined the kinetics of Akt activation following axotomy. In addition, Akt phosphorylation in axotomized retinas was reduced by injection of wortmannin, a PI3K inhibitor, to elucidate the functional significance of Akt activation in axotomized retinas.

* Corresponding author. Department of Anatomy, The University of Hong Kong, 1/F, Laboratory Block, 21 Sassoon Road, Hong Kong, China. Fax: +852-28176821.
E-mail address: hrmaskf@hkucc.hku.hk (K.-F. So).
Available online on ScienceDirect (www.sciencedirect.com.)

1044-7431/$ - see front matter © 2004 Elsevier Inc. All rights reserved.
doi:10.1016/j.mcn.2003.11.001

Results

Cell death profile of axotomized RGCs in hamsters

The number of surviving RGCs at 2, 3, 5, 7, 10, and 14 dpa was determined from flat-mounts and retinal sections. The number of labeled RGCs at 1 dpa was not counted because the dye had not sufficiently reached the RGC soma, which might result in underestimation of the surviving RGCs. Surviving Fluoro-gold (FG)-labeled RGCs were recognized by the fine, grainy, and even distributions of FG staining. Cells exhibiting clumping of FG in the cytoplasm, or cells containing potential phagocytic vacuoles represented by dense rounded vesicles filled with FG were excluded. These are morphologies exhibited by microglia that have engulfed degenerated RGCs (Kacza and Seeger, 1997; Thanos et al., 1994). Fig. 1A shows the morphology of the surviving RGCs and the potential microglia that were excluded from the RGC counts.

Retinal flat-mounts have been used to quantify the number of RGCs following axotomy (Berkelaar et al., 1994; Cho et al., 1999; Villegas-Perez et al., 1993). In the present study, sampling using retinal flat-mounts revealed that RGC loss was already observed at 3 dpa. If we assume the number of surviving RGCs at 2 dpa to represent the number of FG-labeled RGCs in undamaged retina, 36.38% of the total RGCs were lost within 3–5 dpa, representing the fastest RGC loss period following axotomy. Cell loss continued from 5 to 7 dpa, when 24.41% of total RGCs was eliminated. By 10 and 14 dpa, 16.97% and 9.4% of axotomized RGCs remained, respectively. A similar death profile was observed using retinal sections (Fig. 1B). This suggests that the protocol adopted to determine the number of labeled cells in retinal sections provides results comparable to that obtained with a well-established protocol using retinal flat-mounts. The result indicates that our protocol for quantifying stained cells in retinal sections is reliable and applicable.

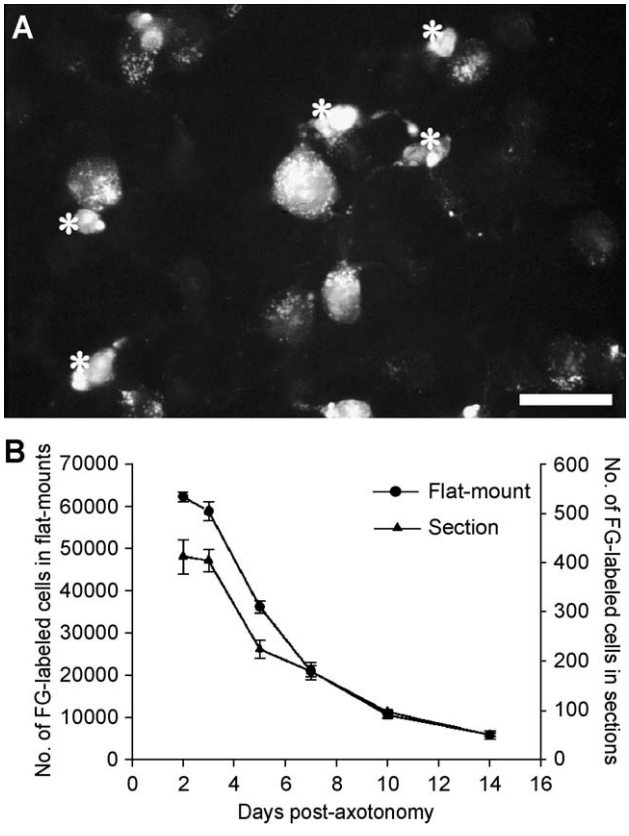

Fig. 1. Loss of RGCs following axotomy. (A) A photomicrograph of a retinal flat-mount at 7 dpa showing the Fluoro-Gold-labeled RGCs and the potential microglia (*), which were excluded from the RGC counts. Scale bar = 25 μm. (B) Temporal profile of RGC loss following axotomy determined from both flat-mounts and retinal sections.

Cleavage of procaspase-9 at Asp353, caspase-3 activation, and nuclear fragmentation not observed until 3 dpa

The kinetics of nuclear fragmentation, activation of caspase-9 and caspase-3 in axotomized retinas were examined. Fragmented nuclei were recognized by the presence of small, rounded and highly fluorescent DAPI-stained entities, which were readily distinguished from normal nuclei based on the size, shape, and intensity of the DAPI-stained nuclei. In addition, an earlier study examining the co-localization of TUNEL staining and nuclear fragmentation based on DAPI staining revealed that the two provided similar results (Isenmann et al., 1997), further establishing the use of nuclear morphology as the indicator of apoptotic nuclear changes. Activation of caspases, on the other hand, was determined by the presence of activated caspase-3 or -9 immunoreactivity.

No activation of caspase-9 was observed at 1 or 2 dpa, and in control retinas (Fig. 2A). Similarly, no activated caspase-3 immunoreactivity or fragmented nucleus was observed in control retinas and on the first 2 days after axotomy. Fragmented nuclei and activated caspase-3 and -9 immunoreactivities first appeared at 3 dpa. The number of cells with fragmented nuclei decreased thereafter, with concomitant decrease in the number of activated caspase-3- and -9-positive cells (Fig. 2A). On the other hand, activated caspase-3 and -9 immunoreactivities were found exclusively in the GCL. Of the activated caspase-3-positive cells, over 90% displayed fragmented nuclei and over 80% were FG-positive at all time-points (Figs. 2B and C). All of the activated caspase-9-positive cells displayed nuclear fragmentation and over 80% of them contained FG-staining (Figs. 2D and E). These observations suggest that most of the cells exhibiting caspase activation were axotomized RGCs. Staining of retinal sections without FG-labeling provided similar results, suggesting that FG-labeling did not interfere with the immunohistochemical staining. Our data indicate that activation of caspases and nuclear fragmentation was delayed by 3 days after axotomy, coinciding with the onset of axotomized RGC death.

The activated caspase-3 immunoreactivity was caspase-9-dependent

To elucidate the causal relationships between the caspase-3 and -9 activation observed following axotomy, we investigated if the activated caspase-3 immunoreactivity was dependent on caspase-9 activation. LEHD-cho and z-LEHD-fmk, the reversible and irreversible caspase-9 inhibitors, function as competitive substrates for the activated enzyme to inhibit its activity (Garcia-Calvo et al., 1998; Thornberry et al., 1997). Intravitreal injection of LEHD-cho and z-LEHD-fmk has been shown to significantly reduce caspase-9 activity at 3 dpa in the axotomized retinas (Kermer et al., 2000a), suggesting that the dosage adopted could effectively inhibit cas-

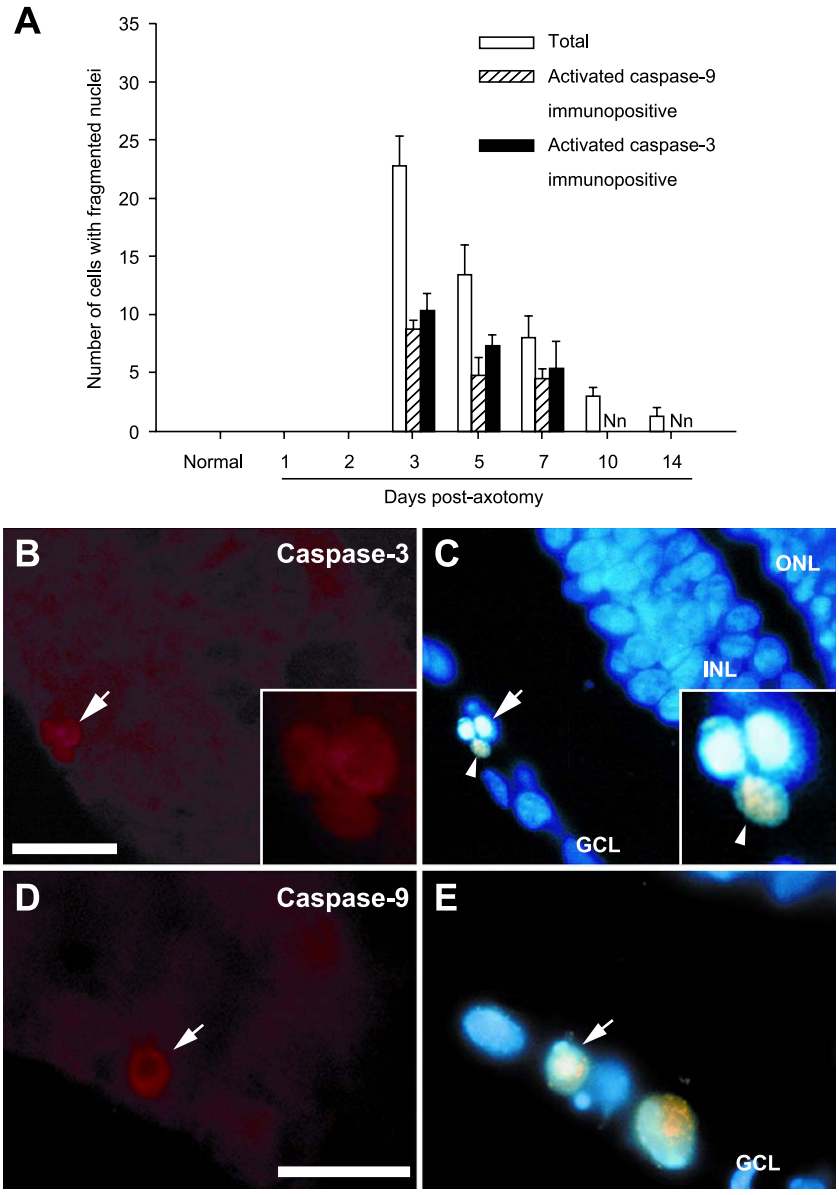

Fig. 2. Immunohistochemical analysis of nuclear fragmentation, caspase-3 and caspase-9 activation following axotomy. (A) The number of cells displaying fragmented nuclei, both nuclear fragmentation and activated caspase-3 immunoreactivity or both nuclear fragmentation and activated caspase-9 immunoreactivity. No nuclear fragmentation, activation of caspase-3 or caspase-9 was detected in normal retinas or in axotomized retinas at 1 and 2 dpa. Caspase-3 activation, caspase-9 activation and nuclear fragmentation were first observed at 3 dpa, and decreased thereafter (N = caspase-9 immunoreactivity not determined; n = capsase-3 immunoreactivity not determined). (B and C) Photomicrographs of the same retinal section stained with activated caspase-3 polyclonal antibody (B) and DAPI (C) at 7 dpa examined under epifluorescence. Note that the cell stained positive for activated caspase-3 was found in the GCL (B and C, arrow). Examination of the same cell under UV-filter revealed that the cell has been broken down into apoptotic bodies (C, arrow), with one still containing remnants of FG staining (Insert, arrowhead). This suggests that the stained cell was a Fluoro-Gold-positive RGC. Insert in B and C: the stained cell at higher magnification. (D and E) Photomicrographs of the same retinal section stained with activated caspase-9 polyclonal antibody (D) and DAPI (E) at 5 dpa. Note that the caspase-9-positive cell (D, arrow) exhibited nuclear fragmentation and was identified as a RGC by the FG staining (E, arrow). Scale bar = 25 μm. ONL: outer nuclear layer; INL: inner nuclear layer; GCL: ganglion cell layer.

pase-9 activity. We found that both inhibitors reduced nuclear fragmentation/condensation by 35–40% at 3 dpa when injected intravitreally (Fig. 3A). This suggests that caspase-9 activation partially mediated the axotomy-induced RGC apoptosis. In addition, caspase-9 inhibitors injections markedly decreased the number of cells with activated caspase-3 immunoreactivity (Fig. 3B), indicating that the activation of caspase-3 in axotomized RGCs was mostly caspase-9 dependent. In accordance with the mechanism of inhibition by these inhibitors, treatment with LEHD-cho and z-LEHD-fmk had no effect on the incidence of activated caspase-9 immunoreactivity at 3 dpa (data not shown). Taken together, our data indicate that the axotomy-induced caspase-3 activation and nuclear fragmentation/condensation were partially due to caspase-9 activation.

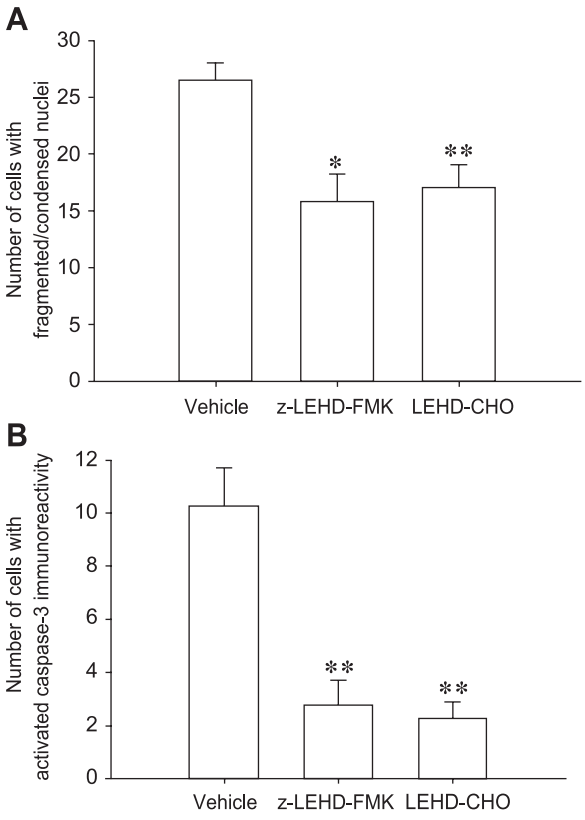

Fig. 3. Caspase-9 inhibitors reduced nuclear fragmentation and caspase-3 activation at 3 dpa. (A) Injections of the irreversible (LEHD-CHO) and reversible (z-LEHD-FMK) caspase-9 inhibitors significantly reduced the number of cells with nuclear fragmentation at 3 dpa. This suggests that activation of caspase-9 played a role in the final demise of the axotomized RGCs. (B) Injections of the reversible and irreversible caspase-9 inhibitors markedly decreased the number of cells with caspase-3 immunoreactivity, indicating that most of the caspase-3 activation observed was dependent on caspase-9 activity. *$P < 0.05$ vs. vehicle-treated group; **$P < 0.01$ vs. vehicle-treated group; one-way ANOVA.

Akt activation increased transiently following axotomy

Since caspase activation was delayed by several days following axotomy, we examined if the PI3K/Akt pathway was implicated in the inhibition of caspase activation in axotomized retinas. Activation of Akt downstream of PI3K via phosphorylation at Serine 473 and Threonine 308 has been shown to serve as an important survival signal for neurons (reviewed in Brazil et al., 2002; Brunet et al., 2001). In addition, Akt has been shown to inhibit the activation of caspase-3 and -9 (Zhou et al., 2000). The activation of the PI3K/Akt pathway may hence take part in delaying the activation of caspases observed in axotomized retinas. We investigated the levels of Akt and the active form of Akt, phospho-Akt (pAkt), at various time-points after axotomy. Western blot analysis revealed that Akt levels remained unchanged up to 7 days post-axotomy (Fig. 4A). Phospho-Akt levels, on the other hand, increased as early as 3 h post-axotomy, peaked at 1 dpa, and remained elevated through 2 dpa (Figs. 4A and B). Akt phosphorylation returned to control level on day 3, when caspases were activated and RGC death commenced. The change in pAkt level thus correlated with the RGC death profile: cell death was inhibited when pAkt level was high; apoptosis proceeded when pAkt level returned to control level.

To verify if the changes in pAkt level was attributed to changes in retinal ganglion cells, immunohistochemical staining against phospho-Akt was performed on control and axotomized retinas. We found that localization of phospho-Akt immunoreactivity remained unchanged following axotomy and was observed only in the GCL in both control and axotomized retinas at 2 dpa (Figs. 4C and D). This suggests that the axotomy-induced upregulation in Akt phosphorylation was mainly localized to the GCL.

Wortmannin or LY294002 injections induced the presence of caspase-3- and -9-positive cells with apoptotic nuclei at 2 dpa

To elucidate the functional significance of the elevated pAkt levels following axotomy, intravitreal injections of 0.1 mM wortmannin (WM) or 1 mM LY294002 (LY) was performed. Both WM and LY are specific inhibitors of PI3K (Davies et al., 2000; Vlahos et al., 1994) and have been shown to lower pAkt levels in control retinas upon intravitreal injections (Kermer et al., 2000b). As expected, WM and LY injections significantly lowered pAkt levels in axotomized retinas relative to that of the vehicle-injected groups (Fig. 5A).

Quantification of the incidence of nuclear fragmentation in the GCL revealed that no fragmented nucleus was observed in the sham-operated group. WM and LY injection, on the other hand, resulted in low levels of nuclear fragmentation in the GCL of unoperated retinas (Fig. 5B). Given the pivotal role of PI3K/Akt in neuronal survival, it is not surprising that reduction in Akt phosphorylation following injection of WM and LY resulted in slightly enhanced nuclear fragmentation in the absence of axotomy. While nuclear fragmentation was not detected in uninjected retinas at 2 dpa (see Fig. 2A), injection of vehicle led to the presence of a few apoptotic nuclei in one of the animals on day 2 post-axotomy. Interestingly, WM injections markedly increased the abundance of fragmented nuclei compared to the vehicle-injected group. LY294002 injections also resulted in a significant increase in nuclear fragmentation, although to a lesser extent compared to the WM-injected group (Figs. 5B and C–E). The discrepancy in the enhancement of nuclear fragmentation between the WM- and LY-injected groups was possibly due to an exceptionally high density of nuclear fragmentation in one of the WM-injected animals (density of 15.5 cells per mm^2 vs. the mean of 6.2 cells per mm^2 for the other three animals). Note that the frequency of nuclear fragmentation induced by WM and LY in axotomized retinas was significantly higher than those in normal retinas (Fig. 5B). The marked increase in nuclear fragmentation in axotomized retinas following suppression of Akt activation suggests that pAkt elevation is particularly crucial for RGC survival following axotomy. Our data indicate that partial inhibition of Akt activation was associated with a premature onset of apoptosis on day 2 post-axotomy, suggesting that PI3K activity and/or enhanced Akt phosphorylation after axotomy may serve as an endogenous protective mechanism to counteract the insult-triggered death signals.

To examine if the WM or LY-induced apoptotic cells in axotomized retinas exhibited caspase activation, WM- or LY-injected eyeballs were cut into frozen sections and subjected to immunohistochemistry against activated caspase-3 and -9. DAPI staining of frozen sections confirmed that fragmented nuclei was present only in the GCL and was not observed in all other layers of

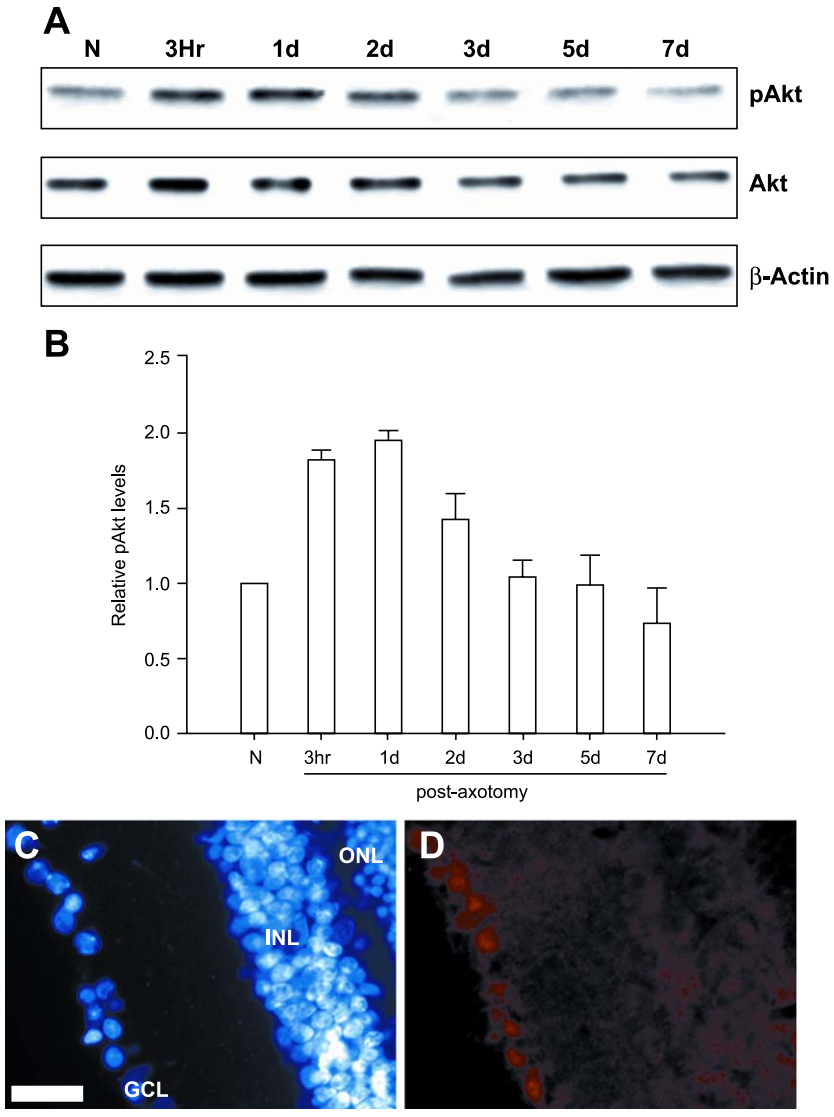

Fig. 4. Phosphorylation of Akt following axotomy. (A) Western blot analysis of the changes in phospho-Akt levels in axotomized retinas. An increase in the phosphorylated form of Akt at serine 473 can be detected as early as 3 h after axotomy. The level of pAkt peaked at 1 dpa and remained high through day 2. Akt levels remained unchanged following axotomy. The expression of β-actin was included to show that equivalent amounts of protein were present in each lane. Representative results from three independent experiments performed in duplicates are shown. (B) A histogram representing the changes in phospho-Akt levels at various time-points after axotomy. (N = normal; Hr = hours post-axotomy; d = day(s) post-axotomy). (C and D) Photomicrographs of the same retinal section stained with DAPI (C) and phospho-Akt antibody (D) at 2 dpa. Note that phospho-Akt staining was observed mostly in the GCL. Scale bar = 25 μm. ONL: outer nuclear layer; INL: inner nuclear layer; GCL: ganglion cell layer.

the retina for both WM- and LY-injected retinas. In addition, morphology of fragmented nuclei was indistinguishable between WM- and LY-injected retinas (data not shown). We found that of all the WM-induced apoptotic nuclei that were examined, 73% of them stained positive for activated caspase-3 (Figs. 5E and F) and 95% of them stained positive for activated caspase-9 (Figs. 5G and H). On the other hand, 66% of the LY-induced fragmented nuclei stained positive for activated caspase-3 and all exhibited caspase-9 activation (data not shown). We therefore showed that WM and LY injections induced caspase-3 and -9 activation in the GCL, resulting in the presence of fragmented nuclei at 2 dpa. Taken together, we believe that the PI3K/Akt pathway may contribute to the delay in caspase-3 and -9 activation following axotomy, and the late onset of RGC death, by inhibiting activation of caspase-9 or -3.

Discussion

Activation of caspases and axotomized RGC death proceeded at a faster rate in hamsters

Most of the earlier studies examining the apoptotic changes in axotomized RGCs have been carried out in rats. To facilitate comparison with previous studies, we characterized the temporal profile of axotomized RGC death in hamsters. In this study, we found that axotomized RGC loss in hamsters progressed at a faster rate compared to that in rats. Where only about 35% of the axotomized RGCs is lost from 2 to 7 dpa in rats (Peinado-Ramon et al., 1996), more than 65% were lost in hamsters. Maximal RGC loss was detected between day 3 and day 5 in hamsters, while it

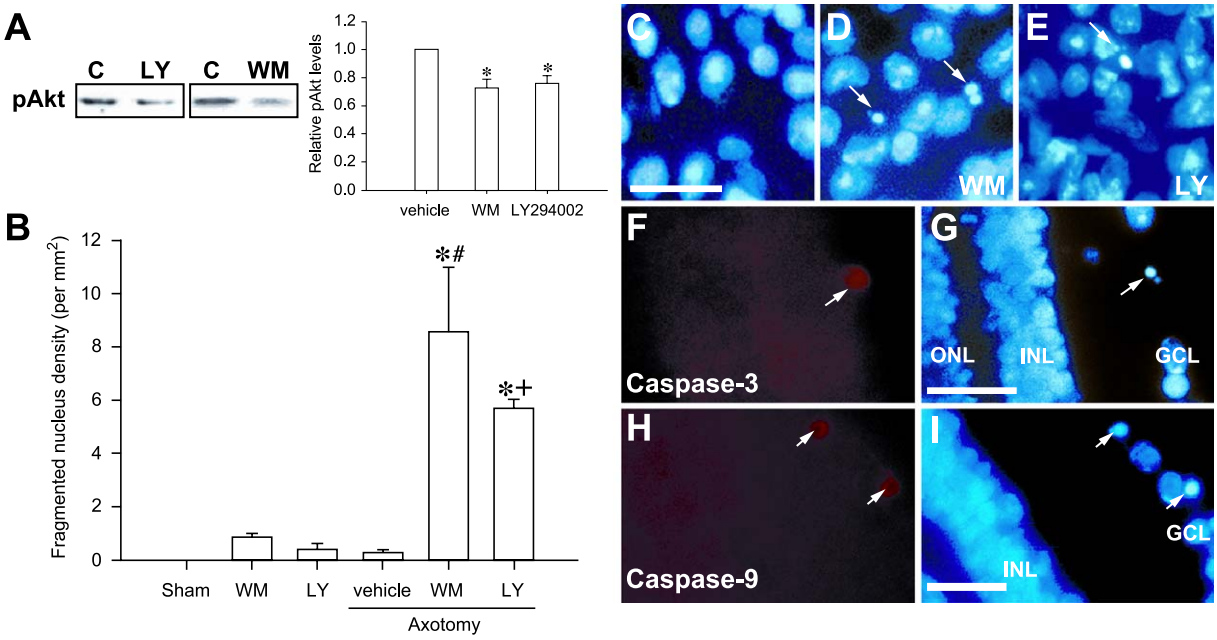

Fig. 5. The effect of wortmannin and LY294002 on pAkt levels, nuclear fragmentation and activation of caspase-3 and -9 in axotomized retinas at 2 dpa. (A) Western blot analysis revealed that injection of wortmannin (WM) and LY294002 (LY) significantly reduced pAkt levels in axotomized retinas at 2 dpa. C = vehicle-injected retina. (B) Injection of WM and LY induced the presence of fragmented nuclei at 2 dpa. No fragmented nuclei were observed in sham-operated group although injection of vehicle led to the presence of a few apoptotic nuclei in one of the retinas. WM and LY injections, however, significantly increased the number of fragmented nuclei at 2 dpa. WM and LY injections in unoperated retinas induced a low level of nuclear fragmentation, but was significantly less than that observed in WM and LY-injected axotomized retinas. (C–E) Photomicrographs of retinal flat-mounts at the level of GCL stained with DAPI injected with vehicle (C), 0.1 mM WM (D) or 1 mM LY (E). Injections of WM and LY led to the presence of apoptotic nuclei (D and E, arrows) in the GCL. Examination of these fragmented nuclei with immunohistochemistry against activated caspase-3 (E and F) and activated caspase-9 (G and H) using retinal sections revealed that caspase-3 or caspase-9 was activated in these cells. F and H are photomicrographs of the retinal section in E and G respectively stained with DAPI. Sections were taken from WM-injected retinas at 2 dpa. Our data indicate that when pAkt level was reduced by WM and LY injections, cells exhibiting fragmented nuclei and caspase-3 or -9 activation were induced in the GCL. Scale bar = 25 μm. *$P < 0.05$ vs. vehicle-treated group, #$P < 0.05$ vs. WM only group; +$P < 0.05$ vs. LY only group. One-way ANOVA.

occurs between day 5 and day 7 in rats (Koeberle and Ball, 1998; Peinado-Ramon et al., 1996; Villegas-Perez et al., 1993). In addition, previous studies have shown that axotomized RGC death does not commence until 4 dpa in rats (Berkelaar et al., 1994). Our study showed that RGC loss began at 3 dpa in hamsters as evidenced by the initial appearance of fragmented nuclei at 3 dpa.

Concomitantly, caspase-3/-9 activation in the GCL was also observed on day 3. No caspases activation was observed at 1 and 2 dpa, indicating that caspase activation was delayed after axonal damage. Our observations corroborate and extend findings from previous studies demonstrating activation of caspase-3 and -9 in axotomized rat retina (Kermer et al., 1999). By examining the temporal profile of caspase activation following axotomy, we verified that caspase activation was not observed before 3 dpa. In addition, we validated the stained cells in the GCL to be RGCs by retrograde labeling. However, we did not observe activation of caspase-3 in the photoreceptors, as was reported by Kermer et al. (1999). The discrepancy could be due to interspecies difference, or difference in the sensitivity or specificity of the antibodies used in the two studies. According to Putcha et al. (1999), the antibody used in Kermer et al.'s study may also recognize activated caspase-7.

The high correlation of nuclear fragmentation and activated caspase-3/-9 immunoreactivity observed in the current study suggests that these two caspases play a role in the morphological changes associated with apoptosis in axotomized RGCs. This observation is in agreement with previous findings showing that caspase-3 cleaves substrates including PARP and fodrin, contributing to the morphological hallmarks of apoptosis such as DNA fragmentation and plasma membrane blebbing (Lazebnik et al., 1994; Martin et al., 1995; Tewari et al., 1995). In addition, our data also suggest that the delayed activation of caspases may contribute to the observed late onset of axotomized RGC death. However, it should be noted that only about 50% of the fragmented nuclei stained positive for activated caspase-3 at all time-points examined in the current study. In addition, caspase-9 inhibitors were more effective in lowering caspase-3 activation than inhibiting nuclear fragmentation. These observations suggest that other pathways may be recruited to eliminate axotomized RGCs; thus, inhibition of caspase-9, despite reducing caspase-3 activation by 80%, was only partially effective in preventing nuclear fragmentation. In agreement with this hypothesis, implication of caspase-8 in axotomized RGC death is recently demonstrated (Weishaupt et al., 2003). Finally, it is important to note that since caspase-9 shares substrate specificity with caspase-4 and -5 (Thornberry et al., 1997), the caspase-9 inhibitors used here may also inhibit caspase-4 and -5. Therefore, the precise involvement of caspases aside from caspase-3 and -9 in the elimination of RGCs following axotomy

is far from clear and further experiments will be required for clarification.

Involvement of the PI3K/Akt pathway in delaying the activation of caspases

Since the kinetics of caspases activation correlated with that of axotomized RGC death, processes implicated in the regulation of caspases activation may also participate in modulating the kinetics of axotomized RGC death. In the current study, we investigated the importance of the PI3K/Akt pathway in the delayed activation of caspases observed in axotomized RGCs. Akt phosphorylation at Serine 473 and Threonine 308, which leads to its activation, occurs downstream of PI3K activation in response to trophic factors (Brunet et al., 2001). Activated Akt effectuates the neuroprotective effect of trophic factors by upregulating the transcription of anti-apoptotic proteins such as Bcl-2 (Pugazhenthi et al., 2000), or by downregulating the expression of death-associated genes (Brunet et al., 1999). Akt has also been shown to phosphorylate Bad, thereby causing it to dissociate from Bcl-x_L to limit cytochrome *c* release (Datta et al., 1997). In support of a neuroprotective role of PI3K/Akt in vivo, exogenous IGF and BDNF have been shown to delay axotomized RGC death by activating the PI3K/Akt pathway (Kermer et al., 2000b; Klocker et al., 2000).

In this study, we found a rapid but transient increase in Akt phosphorylation at 3 h post-axotomy. We subsequently showed that partial inhibition of this increase by WM or LY294002 prompted some cells in the GCL to commit apoptosis at an earlier time-point, implicating the PI3K/Akt pathway in the regulation of RGC apoptosis. Earlier activation of caspase-3 and -9 was demonstrated to take part in this premature apoptosis, indicating that the regulation of RGC death was achieved by limiting caspase activation. The drop in pAkt level on day 3 coincided with the onset of caspase activation and nuclear fragmentation at 3 dpa, suggesting that the lowered pAkt level may contribute to the continuation of the apoptotic cascades on day 3. These observations indicate that Akt phosphorylation may attenuate RGC death by limiting caspase activation in axotomized retinas. However, it should be noted that the use of WM or LY294002 provides no information on the relative importance of PI3K and Akt activation in the inhibition of caspases. PI3K can potentially inhibit caspase activation via other signaling molecules. Nonetheless, the reduction in phospho-Akt levels by WM and LY 294002 injection suggests that Akt may at least mediate some of PI3K's anti-apoptotic effect. The definitive involvement of Akt in the axotomized RGCs awaits the development of Akt-specific inhibitor. Taken together, our data suggest that PI3K activity and/or the axotomy-induced increase in pAkt level may play a physiological role in attenuating RGC apoptosis by inhibiting activation of caspase-3 and/or -9.

A previous study examining Akt phosphorylation following axotomy showed that axotomy leads to a drop in pAkt level on day 4 in rats (Kermer et al., 2000b). In the current study, we similarly observed a slight decrease in pAkt level following axotomy at 5 and 7 dpa, but the decrease was to a lesser extent. By examining the time-points before RGC death, we established that an increase in Akt phosphorylation preceded the lower pAkt content observed on days 5 and 7. Our data corroborate and extend findings from previous reports where apoptotic stimuli are shown to induce an increase in Akt activation (Murashov et al., 2001; Tang et al., 2001; Wang et al., 2000). We have further shown that inhibiting this increase possibly attenuated the kinetics of apoptosis in vivo, providing evidence for the physiological relevance of this increase. The automatic initiation of anti-apoptotic machinery in the face of insults may serve as a built-in fail-safe mechanism to avoid apoptosis of the damaged cells.

The site at which the PI3K/Akt pathway exerted its anti-apoptotic effect in axotomized retinas remains unresolved. In the current study, wortmannin and LY294002 injection induced premature activation of both caspase-3 and -9. Since caspase-3 activation in axotomized RGCs occurred downstream of caspase-9 activity, the concomitant sensitivity of caspase-9 and -3 to wortmannin and LY294002 injection indicates that the PI3K/Akt pathway possibly inhibited caspase activation at the site of caspase-9 activation and/or upstream of caspase-9 activation. Indeed, the PI3K/Akt pathway has been observed to regulate the activation of caspases by modulating upstream events such as cytochrome *c* release (Kennedy et al., 1999). In addition, Akt exerts direct inhibitory effect on both inactive and active forms of human caspase-9 via phosphorylation at Serine 196 (Cardone et al., 1998). Although a previous report showed that the Akt phosphorylation site on human caspase-9 is absent in various mammals including rat and mouse (Fujita et al., 1999), a recent study showed that Akt can block caspase-3 and -9 activation in the presence of microinjected cytochrome *c* in a cell line expressing mouse caspase-9 (Zhou et al., 2000). It is thus possible that PI3K/Akt may directly affect the activation of caspase-9 via other yet unidentified mechanisms. Furthermore, whether the Akt phosphorylation site is present in the hamster caspase-9 remains to be elucidated. Finally, it cannot be ruled out that the PI3K/Akt

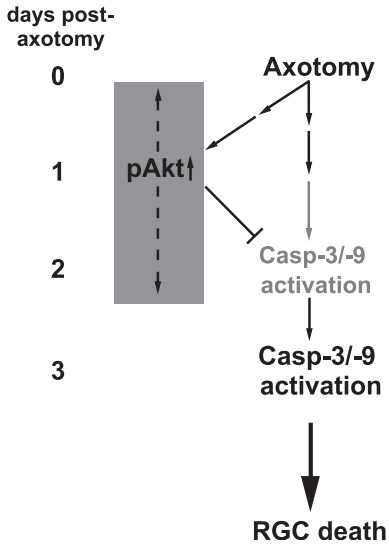

Fig. 6. Schematic diagram illustrating the temporal sequence of Akt activation and caspase activation in axotomized retinas. Axotomy induced a rapid elevation in phospho-Akt (pAkt) at 3 h post-axotomy. Activation of caspase-3 and -9 (casp-3/-9) was delayed by 3 days following axotomy. Our data showed that Akt phosphorylation and/or PI3K activity may contribute to delaying the activation of caspase-3 and -9 to day 3 post-axotomy by inhibiting their activation. When pAkt level returned to control level on day 3, caspase activation proceeded and resulted in the concomitant presence of apoptotic nuclei and RGC death.

pathway may also exhibit direct inhibitory effect on caspase-3, independent from caspase-9 activity. Delineating these possibilities will expand our understanding on the regulation of caspase activity in axotomized retinas, and thus increase our ability to design effective treatments for degenerating RGCs in diseases like glaucoma.

In conclusion, findings from this study demonstrated that caspase-3 and -9 activation and nuclear fragmentation occurred with a delay of 3 days following axotomy, coinciding with the beginning of RGC death post-axotomy. Elevated levels of phospho-Akt were observed as early as 3-h post-axotomy. Partial inhibition of the PI3K/Akt pathway contributed to premature onset of nuclear fragmentation, accompanied by the early activation of caspase-3/-9 in the GCL. These observations suggest that the activation of the PI3K/Akt pathway may be implicated in preventing the activation of caspase-3 and -9 and delaying the onset of caspase-induced apoptosis to 3 dpa (Fig. 6). Our data suggest that the apoptotic stimulus-induced elevation of Akt activation may play a physiological role in preventing the activation of caspases in vivo. Extending the period of elevated Akt phosphorylation, for example, may serve as a feasible treatment for protecting axotomized RGCs or in diseases such as glaucoma.

Experimental methods

Optic nerve transection

A total of 142 adult golden hamsters (*Mesocricetus auratus*, 6–8 weeks old, weighing 60–80 g) were used in this study. All operations were carried out in animals anesthetized with intraperitoneal injection of sodium pentobarbital (Nembutal, Rhone Merieux Australia Pty Ltd., Australia; 50 mg/kg). Unilateral optic nerve transection at 1.5 mm from the optic disc was performed as previously described (Cheung et al., 2002). Surviving RGCs were retrogradely labeled by placing a piece of Gelfoam (Upjohn, Kalamazoo, MI) soaked with 6% Fluoro-Gold (FG; Fluorochrome, Denver, CO) at the ocular stump immediately after the operation. Care was taken to keep the blood supply to the retina intact throughout the operations. Animals with compromised blood supply after the operation, as determined by examining the fundus under an operating microscope, were excluded. Operated animals were sacrificed with an overdose of anesthesia, followed by transcardial perfusion with 4% paraformaldehyde (PFA).

Quantification of surviving RGCs at various time points following axotomy

To examine the death profile of axotomized RGCs, the left eyes of the euthanized animals were enucleated at 1, 2, 3, 5, 7, 10, and 14 days post-axotomy (dpa; $n = 4–6$ per group). The retinas were dissected in 4% PFA and prepared as flat-mounts as previously described (Cheung et al., 2002). Flat-mounted retinas were examined under fluorescence microscopy using an ultra-violet filter (excitation wavelength = 330–380 nm). Labeled RGCs were counted along the median line of the four quadrants starting from the optic disc to the peripheral border of the retina at 500-μm intervals, under an eyepiece grid of 200 × 200 μm. The mean density of labeled RGCs in each retina was then multiplied by the area of the retina to obtain the number of labeled RGCs in the retina.

Immunohistochemistry

The left eyes of all animals prepared for immunohistochemical analysis were enucleated following transcardial perfusion with 4% PFA and subsequently post-fixed in the same fixative for 4 h. Ten-micron-thick frozen sections were cut with a Leica cryomicrotome. The sections were cut transversely along the superior–inferior axis of the eyeball and stored at −20 °C until use. Only sections containing the optic nerve stump were used in this study to ensure comparability.

For immunohistochemical detection of activated caspase-3 and activated caspase-9, animals were divided into three subgroups: (1) unoperated animals to serve as control ($n = 4$); (2) animals that have received optic nerve transection and FG-labeling of RGCs, sacrificed at 1, 2, 3, 5, 7, 10, and 14 dpa ($n = 4–5$ per group); (3) animals that have received axotomy without FG-labeling, sacrificed at 1, 2, 3, and 5 dpa ($n = 4$). Animals in group 3 served as negative controls to verify independence of the immunohistochemical staining from FG interference.

Retinal sections were thawed, air-dried, and washed three times in 0.1 M phosphate-buffered saline (PBS, pH 7.4). The sections were first blocked with 3% normal goat serum (NGS) in 0.3% Triton X-100 at room temperature for 20 min. The slides were then incubated with anti-activated caspase-3 polyclonal antibody (1:150; Cell Signaling Technology, Beverly, MA) or anti-activated caspase-9 polyclonal antibody (1:100; Cell Signaling Technology) in NGS and 0.3% Triton X-100 overnight at 4 °C. After rinsing, activated caspase-3 and activated caspase-9 staining was visualized by texas red-conjugated goat anti-rabbit secondary antibody at 1:50 (Vector Laboratories, Berlingame, CA). All slides were counterstained with 4,6-diaminido-2-phenylindole (DAPI; Sigma, St. Louis, MO) to reveal nuclear morphology. Processed slides were coverslipped using Vectashield® mounting medium for fluorescence (Vector laboratories) and examined under epifluorescence.

Counting of labeled RGCs, activated caspase-3 and -9 immunoreactivity in sections

The number of FG-labeled RGCs, texas red-positive cells (for activated caspase-3 or -9) and fragmented nuclei in each retinal section was counted. The number of cells exhibiting co-localization of any two of the mentioned parameters was also counted. Counting was done on three retinal sections per animal to increase the reliability of the data. The numbers counted from the three sections were added up to give the final number of labeled cells in each retina. Since all the retinal sections used in this study contained the optic nerve stump, the length of all the retinal sections was comparable (8399 ± 76 μm). The number of labeled cells in each retinal section was therefore used as an estimation of the labeled cell density. FG-labeled RGCs and DAPI-stained nuclei were examined using an ultra-violet filter (excitation wavelength = 330–380 nm). The colors of the two dyes (yellow for FG and blue-white for DAPI) were readily distinguished from each other under the same filter (Fig. 2E). Fragmented nuclei were identified as described by earlier reports (Darzynkiewics and Traganos, 1998; Isenmann et al., 1997). Briefly, fragmented nuclei were identified as small, rounded

and fragmented nuclear entities that are brightly labeled by DAPI. Nuclear fragmentation and formation of apoptotic bodies are morphologies associated with a late stage of apoptosis (Darzynkiewics and Traganos, 1998). Texas red-stained cells were examined using filters with excitation wavelengths of 510–560 nm (red).

Temporal profile of Akt phosphorylation

To examine the temporal profile of Akt phosphorylation in axotomized retinas, anesthetized animals received axotomy without FG-labeling of RGCs. Operated animals were euthanized at 3 h, 1, 2, 3, 5, and 7 days post-axotomy ($n = 3$ per group). Retinas from the left eyes of three unoperated animals were also dissected to serve as control. Dissected retinas from all groups were snap-frozen with liquid nitrogen and stored at −80°C until Western blotting using primary antibody against phospho-Akt (phosphorylation at Ser473 for Akt1, 1:500, Cell Signaling Technology) or Akt (recognizes Akt1, Akt2, and Akt3; 1:500, Cell Signaling Technology). In addition, immunohistochemical staining against phospho-Akt (phosphorylation at Ser473 for Akt1, 1:150, Cell Signaling Technology) was performed as described using frozen sections of unoperated and axotomized retinas at 2 dpa to examine the localization of phospho-Akt in the retina.

Western blot analysis

Procedures for Western blot analysis were adopted from Klocker et al. (2000) with slight modifications. Retinas were homogenized in lysis buffer (50 mM Tris, 150 mM NaCl, 1% Triton X-100, 10% protease inhibitor cocktail from Sigma and 1% phosphatase inhibitor cocktail from Sigma) and lysed on ice for 20 min. Following centrifugation at 13,000 rpm for 15 min to pellet cell debris, the protein concentration of the supernatant was measured using BCA reagent (Pierce, Rockford, IL). Eighty micrograms of retinal lysates were then separated by reducing SDS-PAGE and transferred onto nitrocellulose membrane. The membranes were briefly washed and blocked with 5% skim milk in Tris-buffered saline containing 0.05% Tween 20 (TBST) for 2 h in room temperature. Incubation with primary antibody in 5% skim milk in TBST was performed overnight at 4°C. Subsequently, the membranes were again washed with TBST and incubated with HRP-conjugated secondary antibody for 1 h in room temperature, followed by detection using the SuperSignal® West Pico Chemiluminescent Substrate kit (Pierce). The chemiluminescence was captured by the UVP-Chemi system and the intensity of each band was analyzed using the LabWorks™ Image acquisition and Analysis Software (UVP Inc., Upland, CA). All experiments for Western blotting were performed with three animals in each group and repeated twice. Selected blots were directly reprobed with anti-β-actin antibody (1:5000; Sigma) as previously described to ensure even loading and transfer of samples (Liao et al., 2000).

Intravitreal injections of caspase-9 inhibitors and wortmannin

Wortmannin (WM; Sigma), LY294002 (LY; Calbiochem), reversible (LEHD-CHO; Calbiochem, San Diego, CA) and irreversible (z-LEHD-FMK; Calbiochem) caspase-9 inhibitors were dissolved in 100% dimethylsulfoxide (DMSO; Sigma) and subsequently diluted to the final concentrations using sterile PBS. Intravitreal injections were performed using glass micropipettes at about 1 mm towards to optic nerve from the superior scleral–conjunctival junction of the operated eye.

To examine the effect of caspase-9 inhibitors on nuclear fragmentation and activated caspase-3 immunoreactivity, animals were injected with vehicle (4% DMSO, 4 μl; $n = 4$) LEHD-CHO (4 μg; $n = 4$) or z-LEHD-FMK (4 μg; $n = 4$) immediately after axotomy (day 0) and on day 2 after axotomy. Animals were sacrificed at 3 dpa and the operated eyeballs were removed and processed for immunohistochemical analysis against activated caspase-3 followed by DAPI staining. The number of cells exhibiting nuclear fragmentation and activated caspase-3 immunoreactivity in each group was counted.

The effects of WM and LY on nuclear fragmentation and caspases activation were examined by injecting 4 μl of 0.1 mM WM, 1 mM LY or vehicle (10% DMSO) immediately after axotomy and at 1 dpa. Wortmannin and LY294002 are specific inhibitors of phosphoinositides 3-kinase (PI3K), an enzyme required for the activation of Akt. Operated animals were sacrificed on day 2 and were divided into three groups: (1) animals whose retinas were flat-mounted and stained with DAPI for quantification of nuclear fragmentation ($n = 16$). A sham-operated group was included in this analysis where the whole thickness of the scleral-retina was punctured using micropipette without injecting any solutions. In addition, WM and LY injections were performed on unoperated animals to examine the cytotoxicity of both drugs 2 days after the initial injection ($n = 6$). Retinal flat-mounts were prepared as previously described. Fixed retinas were washed in PBS and stained with DAPI at a concentration of 0.5 μg/ml for 5 min. The presence of fragmented nuclei in the ganglion cell layer (GCL) was detected by focusing onto the GCL based on the FG staining of RGCs under epifluorescence with an ultra-violet filter. The number of fragmented nuclei was then quantified using the sampling method previously described for counting FG-labeled RGCs in retinal flat-mounts except counting was done under an eyepiece grid of 400 × 400 μm. The enlarged sampling area is required for proper quantification of the scarce WM- and LY-induced apoptotic nuclei. (2) Operated eyeballs were processed for immunohistochemistry against activated caspase-3 and -9 ($n = 9$). Ten-micron frozen sections were obtained along the superiotemporal–inferionasal axis to maximize the probability of locating WM- and LY-induced apoptotic nuclei. The sections were stained with DAPI to visualize the WM- and LY-induced apoptotic cells. The number of cells with fragmented nuclei and activated caspase-3 or -9 immunoreactivity was counted. (3) Retinas from operated eyes were removed and processed for Western blotting to assess the effect of WM and LY injections on Akt activation in axotomized retinas at 2 dpa ($n = 12$) using a primary antibody against phospho-Akt (phosphorylation at Ser473, 1:500; Cell Signaling Technology).

Statistics

Data are given as mean ± standard error of mean (SEM). Statistical significance was evaluated by Student's t test for comparisons between two groups; or by one-way ANOVA, followed by Tukey–Kramer post hoc test for comparisons among three or more groups. Differences were considered significant for $P < 0.05$.

Acknowledgments

The authors would also like to thank Ms. Reiko Cheung and Mr. K.K. Yip for their technical assistance in Western blotting. This research is supported by a research grant from the University of Hong Kong, China, a grant from the Areas of Excellence scheme established under the University Grants Committee of the Hong Kong Special Administrative Region, China (Project AOE/P-10/01) and an ASD grant from the Hong Kong Polytechnic University, China. Z.H. Cheung is supported by a Croucher Foundation Scholarship, Hong Kong.

References

Barber, A.J., Nakamura, M., Wolpert, E.B., Reiter, C.E., Seigel, G.M., Antonetti, D.A., Gardner, T.W., 2001. Insulin rescues retinal neurons from apoptosis by a phosphatidylinositol 3-kinase/Akt-mediated mechanism that reduces the activation of caspase-3. J. Biol. Chem. 276, 32814–32821.

Berkelaar, M., Clarke, D.B., Wang, Y.C., Bray, G.M., Aguayo, A.J., 1994. Axotomy results in delayed death and apoptosis of retinal ganglion cells in adult rats. J. Neurosci. 14, 4368–4374.

Brazil, D.P., Park, J., Hemmings, B.A., 2002. PKB binding proteins. Getting in on the Akt. Cell 111, 293–303.

Brunet, A., Bonni, A., Zigmond, M.J., Lin, M.Z., Juo, P., Hu, L.S., Anderson, M.J., Arden, K.C., Blenis, J., Greenberg, M.E., 1999. Akt promotes cell survival by phosphorylating and inhibiting a Forkhead transcription factor. Cell 96, 857–868.

Brunet, A., Datta, S.R., Greenberg, M.E., 2001. Transcription-dependent and -independent control of neuronal survival by the PI3K-Akt signaling pathway. Curr. Opin. Neurobiol. 11, 297–305.

Cardone, M.H., Roy, N., Stennicke, H.R., Salvesen, G.S., Franke, T.F., Stanbridge, E., Frisch, S., Reed, J.C., 1998. Regulation of cell death protease caspase-9 by phosphorylation. Science 282, 1318–1321.

Chaudhary, P., Ahmed, F., Quebada, P., Sharma, S.C., 1999. Caspase inhibitors block the retinal ganglion cell death following optic nerve transection. Brain Res. Mol. Brain Res. 67, 36–45.

Cheung, Z.H., So, K.F., Lu, Q., Yip, H.K., Wu, W., Shan, J.J., Pang, P.K., Chen, C.F., 2002. Enhanced survival and regeneration of axotomized retinal ganglion cells by a mixture of herbal extracts. J. Neurotrauma 19, 369–378.

Cho, K.S., Chan, P.M., So, K.F., Yip, H.K., Chung, S.K., 1999. Ciliary neurotrophic factor promotes the regrowth capacity but not the survival of intraorbitally axotomized retinal ganglion cells in adult hamsters. Neuroscience 94, 623–628.

Darzynkiewics, Z., Traganos, F., 1998. Measurement of apoptosis. In: Al-Rubeai, M. (Ed.), Apoptosis. Springer, Berlin, pp. 33–74.

Datta, S.R., Dudek, H., Tao, X., Masters, S., Fu, H., Gotoh, Y., Greenberg, M.E., 1997. Akt phosphorylation of BAD couples survival signals to the cell-intrinsic death machinery. Cell 91, 231–241.

Davies, S.P., Reddy, H., Caivano, M., Cohen, P., 2000. Specificity and mechanism of action of some commonly used protein kinase inhibitors. Biochem. J. 351, 95–105.

Dudek, H., Datta, S.R., Franke, T.F., Birnbaum, M.J., Yao, R., Cooper, G.M., Segal, R.A., Kaplan, D.R., Greenberg, M.E., 1997. Regulation of neuronal survival by the serine-threonine protein kinase Akt. Science 275, 661–665.

Fujita, E., Jinbo, A., Matuzaki, H., Konishi, H., Kikkawa, U., Momoi, T., 1999. Akt phosphorylation site found in human caspase-9 is absent in mouse caspase-9. Biochem. Biophys. Res. Commun. 264, 550–555.

Garcia-Calvo, M., Peterson, E.P., Leiting, B., Ruel, R., Nicholson, D.W., Thornberry, N.A., 1998. Inhibition of human caspases by peptide-based and macromolecular inhibitors. J. Biol. Chem. 273, 32608–32613.

Isenmann, S., Wahl, C., Krajewski, S., Reed, J.C., Bahr, M., 1997. Up-regulation of Bax protein in degenerating retinal ganglion cells precedes apoptotic cell death after optic nerve lesion in the rat. Eur. J. Neurosci. 9, 1763–1772.

Kacza, J., Seeger, J., 1997. Transcellular labelling of activated retinal microglia following transection of the optic nerve. Inflamm. Res. 46, 430–433.

Kennedy, S.G., Kandel, E.S., Cross, T.K., Hay, N., 1999. Akt/Protein kinase B inhibits cell death by preventing the release of cytochrome *c* from mitochondria. Mol. Cell. Biol. 19, 5800–5810.

Kermer, P., Klocker, N., Labes, M., Bahr, M., 1998. Inhibition of CPP32-like proteases rescues axotomized retinal ganglion cells from secondary cell death in vivo. J. Neurosci. 18, 4656–4662.

Kermer, P., Klocker, N., Labes, M., Thomsen, S., Srinivasan, A., Bahr, M., 1999. Activation of caspase-3 in axotomized rat retinal ganglion cells in vivo. FEBS Lett. 453, 361–364.

Kermer, P., Ankerhold, R., Klocker, N., Krajewski, S., Reed, J.C., Bahr, M., 2000a. Caspase-9: involvement in secondary death of axotomized rat retinal ganglion cells in vivo. Brain Res. Mol. Brain Res. 85, 144–150.

Kermer, P., Klocker, N., Labes, M., Bahr, M., 2000b. Insulin-like growth factor-I protects axotomized rat retinal ganglion cells from secondary death via PI3-K-dependent Akt phosphorylation and inhibition of caspase-3 In vivo. J. Neurosci. 20, 2–8.

Klocker, N., Kermer, P., Weishaupt, J.H., Labes, M., Ankerhold, R., Bahr, M., 2000. Brain-derived neurotrophic factor-mediated neuroprotection of adult rat retinal ganglion cells in vivo does not exclusively depend on phosphatidyl-inositol-3′-kinase/protein kinase B signaling. J. Neurosci. 20, 6962–6967.

Koeberle, P.D., Ball, A.K., 1998. Effects of GDNF on retinal ganglion cell survival following axotomy. Vis. Res. 38, 1505–1515.

Lazebnik, Y.A., Kaufmann, S.H., Desnoyers, S., Poirier, G.G., Earnshaw, W.C., 1994. Cleavage of poly(ADP-ribose) polymerase by a proteinase with properties like ICE. Nature 371, 346–347.

Liao, J., Xu, X., Wargovich, M.J., 2000. Direct reprobing with anti-beta-actin antibody as an internal control for Western blotting analysis. Biotechniques 28, 216–218.

Martin, S.J., O'Brien, G.A., Nishioka, W.K., McGahon, A.J., Mahboubi, A., Saido, T.C., Green, D.R., 1995. Proteolysis of fodrin (non-erythroid spectrin) during apoptosis. J. Biol. Chem. 270, 6425–6428.

Murashov, A.K., Ul, H.I., Hill, C., Park, E., Smith, M., Wang, X., Goldberg, D.J., Wolgemuth, D.J., 2001. Crosstalk between p38, Hsp25 and Akt in spinal motor neurons after sciatic nerve injury. Brain Res. Mol. Brain Res. 93, 199–208.

Nunez, G., del Peso, L., 1998. Linking extracellular survival signals and the apoptotic machinery. Curr. Opin. Neurobiol. 8, 613–618.

O'Gorman, D.M., Cotter, T.G., 2001. Molecular signals in anti-apoptotic survival pathways. Leukemia 15, 21–34.

Peinado-Ramon, P., Salvador, M., Villegas-Perez, M.P., Vidal-Sanz, M., 1996. Effects of axotomy and intraocular administration of NT-4, NT-3, and brain-derived neurotrophic factor on the survival of adult rat retinal ganglion cells. A quantitative in vivo study. Invest. Ophthalmol. Vis. Sci. 37, 489–500.

Politi, L.E., Rotstein, N.P., Salvador, G., Giusto, N.M., Insua, M.F., 2001. Insulin-like growth factor-I is a potential trophic factor for amacrine cells. J. Neurochem. 76, 1199–1211.

Pugazhenthi, S., Nesterova, A., Sable, C., Heidenreich, K.A., Boxer, L.M., Heasley, L.E., Reusch, J.E., 2000. Akt/protein kinase B up-regulates Bcl-2 expression through cAMP-response element-binding protein. J. Biol. Chem. 275, 10761–10766.

Putcha, G.V., Deshmukh, M., Johnson, E.M., 1999. BAX translocation is a critical event in neuronal apoptosis: regulation by neuroprotectants, BCL-2, and caspases. J. Neurosci. 19, 7476–7485.

Takano, M., Horie, H., 1994. Critical period for degradation of adult rat retinal ganglion cells and their regeneration capability after axotomy. Neurosci. Lett. 175, 129–132.

Tang, D., Okada, H., Ruland, J., Liu, L., Stambolic, V., Mak, T.W., Ingram,

A.J., 2001. Akt is activated in response to an apoptotic signal. J. Biol. Chem. 276, 30461–30466.

Tewari, M., Quan, L.T., O'Rourke, K., Desnoyers, S., Zeng, Z., Beidler, D.R., Poirier, G.G., Salvesen, G.S., Dixit, V.M., 1995. Yama/CPP32 beta, a mammalian homolog of CED-3, is a CrmA-inhibitable protease that cleaves the death substrate poly(ADP-ribose) polymerase. Cell 81, 801–809.

Thanos, S., Kacza, J., Seeger, J., Mey, J., 1994. Old dyes for new scopes: the phagocytosis-dependent long-term fluorescence labelling of microglial cells in vivo. Trends Neurosci. 17, 177–182.

Thornberry, N.A., Rano, T.A., Peterson, E.P., Rasper, D.M., Timkey, T., Garcia-Calvo, M., Houtzager, V.M., Nordstrom, P.A., Roy, S., Vaillancourt, J.P., Chapman, K.T., Nicholson, D.W., 1997. A combinatorial approach defines specificities of members of the caspase family and granzyme B. Functional relationships established for key mediators of apoptosis. J. Biol. Chem. 272, 17907–17911.

Villegas-Perez, M.P., Vidal-Sanz, M., Rasminsky, M., Bray, G.M., Aguayo, A.J., 1993. Rapid and protracted phases of retinal ganglion cell loss follow axotomy in the optic nerve of adult rats. J. Neurobiol. 24, 23–36.

Vlahos, C.J., Matter, W.F., Hui, K.Y., Brown, R.F., 1994. A specific inhibitor of phosphatidylinositol 3-kinase, 2-(4-morpholinyl)-8-phenyl-4H-1-benzopyran-4-one (LY294002). J. Biol. Chem. 269, 5241–5248.

Wang, X., McCullough, K.D., Franke, T.F., Holbrook, N.J., 2000. Epidermal growth factor receptor-dependent Akt activation by oxidative stress enhances cell survival. J. Biol. Chem. 275, 14624–14631.

Weishaupt, J.H., Diem, R., Kermer, P., Krajewski, S., Reed, J.C., Bahr, M., 2003. Contribution of caspase-8 to apoptosis of axotomized rat retinal ganglion cells in vivo. Neurobiol. Dis. 13, 124–135.

Zhou, H., Li, X.M., Meinkoth, J., Pittman, R.N., 2000. Akt regulates cell survival and apoptosis at a postmitochondrial level. J. Cell Biol. 151, 483–494.